

Tough, adhesive, self-healing, fully physical crosslinked κ -CG-K⁺/pHEAA double-network ionic conductive hydrogels for wearable sensors[☆]

Jianxiong Xu^{a,b}, Ziyu Guo^a, Yin Chen^a, Yuecong Luo^a, Shaowen Xie^a, Yutong Zhang^a, Haihu Tan^a, Lijian Xu^{a,b,*}, Jie Zheng^c

^a Hunan Key Laboratory of Biomedical Nanomaterials and Devices, College of Life Sciences and Chemistry, Hunan University of Technology, Zhuzhou, 412007, PR China

^b National & Local Joint Engineering Research Centre of Advanced Packaging Materials Developing Technology, Hunan University of Technology, Zhuzhou, 412007, PR China

^c Department of Chemical, Biomolecular, and Corrosion Engineering, The University of Akron, Akron, OH, 44325, USA

ARTICLE INFO

Keywords:

Conductive hydrogels
Double-network hydrogels
 κ -carrageenan
Adhesiveness
Strain sensor

ABSTRACT

The development of multiple-functional conductive hydrogels with combined merits of high mechanical strength, fast self-healing, strong surface adhesion, and strain sensibility has proved to be a highly demanded, but extremely challenging task for different applications. Herein, we designed, synthesized, and characterized fully physically crosslinked double-network (DN) hydrogels of κ -carrageenan/poly(*N*-hydroxyethyl acrylamide) (κ -CG-K⁺/pHEAA DN gels) using a facile heating-cooling-photopolymerization process. The resultant κ -CG-K⁺/pHEAA gels exhibited highly mechanical (tensile strength of 2.02 MPa, tensile strain of 1550%, and elastic modulus of 0.91 MPa) and self-healing properties owing to the interpenetrating DN structures and reversible hybrid ionic-hydrogen bond cross-linking networks. In parallel to high mechanical properties in bulk, κ -CG-K⁺/pHEAA gels also demonstrated their high surface adhesion of ~ 773 J/m² on different untreated hard substrates (i.e., titanium, aluminum, ceramic, and glass), which stemmed from the rich-functional groups (hydroxyl and amide) in pHEAA polymer chains. Moreover, the DN gels also presented conductivity, strain sensitivity with gauge factor (*GF*) = 2.48, and sensing stability due to the presence of K⁺ and stretching-dependent resistance variations. Such a unique combination of high mechanical, adhesive, and conductive properties in κ -CG-K⁺/pHEAA gels allows us to further fabricate them into gel-based strain sensors with high and rapid sensitivity for detecting subtle strain-induced human motions. The design concept and hydrogel system from this work provide a new angle for broad human-machine interface applications.

1. Introduction

Human-machine interfacial devices have been well recognized for their great impacts on broad applications in artificial intelligence, wearable devices, and soft robotics, clinical medicine [1–5]. Among these devices, smart-soft strain sensors are particularly unique and important due to their deformation capabilities, high strain sensitivity, and stable electrical performance. A general working principle of strain sensors is to convert external force or mechanical deformation into electrical signals of resistance [6], voltage [7], and capacitance [8]. Conventional design strategies for strain sensors are to incorporate conductive metal circuits (e.g., metallic nanowires, metallic nanoparticles, and carbon nanomaterials) or conductive polymers into a

flexible polymer substrate (e.g., polyurethane, polydimethylsiloxane, and polytetrafluoroethylene) [9–11]. However, conventional elastomer-based strain sensors often suffer from poor biocompatibility and limited stretchability, which restrict their detection sensitivity and sensing applications [12].

Conductive hydrogels including carbon-based hydrogels [13], metal oxides-integrated hydrogels [14], conducting polymer hydrogels [15], and ionic hydrogels [16] have received great attention to be fabricated into wearable strain sensors. Among them, ionic hydrogels have additional advantages of high optical transparency, freezing tolerance, and excellent ionic conductivity. Di et al. synthesized ionic conductive hydrogels of poly(vinyl alcohol)-NaCl (PVA-N) by integrating NaCl ions into a physically crosslinked PVA network and used them as strain

[☆] Electronic supplementary information (ESI) available.

* Corresponding author. Hunan Key Laboratory of Biomedical Nanomaterials and Devices, College of Life Sciences and Chemistry, Hunan University of Technology, Zhuzhou, 412007, PR China.

<https://doi.org/10.1016/j.polymer.2021.124321>

Received 10 September 2021; Received in revised form 18 October 2021; Accepted 30 October 2021

Available online 1 November 2021

0032-3861/© 2021 Published by Elsevier Ltd.

sensors to detect different motions of the human body [17]. Sun and co-workers reported ionic polyampholyte (PA) hydrogels consisting of positively charged imidazolium-based ionic liquids and negatively charged 3-sulfopropyl methacrylate potassium salts [18]. The resultant hydrogels demonstrated their high electrical conductivity (≈ 3 S/m) and excellent self-healing capability in wearable electronic sensors for potential application value. The above-mentioned ionic conductive hydrogels represent typical design concepts for conducting hydrogels by simply introducing ionic (salt) agents into polymer networks to empower the conductive property of host materials. While most of the existing conductive hydrogels exhibited superior conductivity (0.002–5.12 S/m) as co-contributed by conducting additives and waters, they still suffered from poor mechanical strength due to the lack of effective mechanical dissipation network structure [19].

The past decade has witnessed the growing interest in double-network hydrogels (DN gels) thanks to their unique network structure and excellent mechanical strength [20]. Among them, fully chemically crosslinked and hybrid physically-chemically crosslinked DN gels are the most commonly synthesized and recognized by their high mechanical properties [21,22] due to the presence of strong covalent bonds in the crosslinked network. However, the irreversible and permanent breakage of chemically cross-linked networks inevitably caused the DN gels to be difficultly recovered or self-repaired from external damages [23]. It is a more challenging task to design and synthesize fully physically crosslinked DN gels with comparable mechanical strength to chemically-crosslinked gels [24,25]. Physical DN gels usually possess intrinsic advantages of better self-healing and self-recovery properties [26,27], which allow to significantly prolong the stability and reliability of strain sensors in different applications [28]. Moreover, hydrogel-based strain sensors used in wearable devices also require surface adhesion properties to any target surface (e.g. solid metal surfaces, soft tissues, and human skin). Surface adhesion of hydrogels to the surfaces is mainly determined by both hydrogel toughness itself and hydrogel-surface interactions (i.e., interfacial toughness) [29,30]. Although most of the fully physically crosslinked DN hydrogels exhibited high bulk toughness (≥ 1 MPa), very few showed high interfacial toughness between the hydrogel and surfaces. Therefore, it remains a challenge to simultaneously achieve both bulk and interfacial toughness of any given hydrogel, presumably because the two toughness stems from different intermolecular interactions.

Recently, polysaccharide-based DN hydrogels [31] including agar/poly(*N*-hydroxyethyl acrylamide) (pHEAA) [30], gelatin/pHEAA [32], agar/poly(acrylic acid)/Fe³⁺ [33], agar/*N*-poly(acryloylaminoethoxyethanol) [34], and polyacrylamide/alginate [35] have been developed to possess both bulk and interfacial toughness. Apart from agar and gelatin as the member of a polysaccharide family, Kappa carrageenan (κ -CG) as an anion polysaccharide is extracted from red seaweeds, exhibits typical thermo-reversible gelation behavior [36], can interact with potassium ions (K⁺) to form an anion complex [37]. Gao et al. have reported the dual physical-crosslinking polyacrylamide/ κ -CG DN gels with rapid self-recovery and self-healing properties for strain sensors, but tensile stress of 0.8 MPa was not as high as conventional DN gels [38]. Fu et al. fabricated κ -CG/P(acrylamide-co-acrylic acid) hydrogels into highly sensitive pressure and strain sensors, with tensile stress of 2.7 MPa, and fracture strain of 1400% [39]. These studies have demonstrated that incorporation of K⁺ into κ -CG not only increases the physical crosslinking density of κ -CG but also endows the gels to electrochemical properties for strain sensitivity. However, these κ -CG-based DN gels are lack of surface adhesion properties, making the sensing stability and reliability of these strain sensors more vulnerable.

Inspired by these limits, here we designed and synthesized fully physical crosslinked κ -CG-based hydrogels made of K⁺ ionically crosslinked κ -CG (κ -CG-K⁺) as the first network and hydrogen bonding crosslinked pHEAA as the second network using a simple heating-cooling-photopolymerization process. The HEAA containing plenty of

amide and hydroxyl groups was selected as monomer of the second polymer network since the functional groups in pHEAA networks can serve as both hydrogen-bonding donors and acceptors that regulate the noncovalent interactions between hydrogel and various surfaces endowing the hydrogels with adhesive properties. Due to the reversible physical bonds and the double-network structure, the resultant κ -CG-K⁺/pHEAA DN gels exhibited not only superior bulk properties of mechanical strength, optical transparency, and self-healing, but also high surface adhesion on different solid surfaces of titanium, aluminum, ceramic, and glass. Moreover, the κ -CG-K⁺/pHEAA DN gels showed stretching-dependent electric resistance with high strain sensibility. Ascribe to its unique combination of superior stretchable, self-adhesive, and ionic-conductivity, the κ -CG-K⁺/pHEAA hydrogels were further fabricated into strain sensors with high sensing stability and robustness for monitoring human motions. This new fully physical hydrogel and hydrogel-fabricated strain sensor, without any conductive fillers, holds great promise for broad human-machine interface applications.

2. Materials and methods

2.1. Materials

κ -carrageenan (κ -CG, >99%), urea (99.5%), sodium thiocyanate (NaSCN, 98%), 2-hydroxy-4'-(2-hydroxyethoxy)-2-methylpropiophenone (Irgacure 2959, UV initiator), and potassium chloride (99.5%) were purchased from Sigma-Aldrich. *N*-Hydroxyethyl acrylamide (HEAA, >98%) was obtained from TCI. Water used in this work was purified by a Millipore water purification system.

2.2. Preparation of κ -CG-K⁺/pHEAA DN hydrogels

The κ -CG-K⁺/pHEAA DN gels were synthesized via a simple one-pot heating-cooling-photopolymerization process [31]. Choosing the DN-G₂₀₀-H₅-K₆ gels as a typical example, 200 mg κ -CG, 5.0 g (0.043 mol) *N*-Hydroxyethyl acrylamide, and 9.7×10^{-2} g UV initiator (1.0 mol% of HEAA) were dissolved in 4 mL deionized water at 95 °C and stirred magnetically to form a homogeneous solution. Subsequently, KCl (6 wt % of κ -CG) was added to the solution and unceasingly stirred until the potassium chloride was completely dissolved. The precursor solution was injected into a 1 mm thick glass mold and cooled to room temperature. Then, the glass mold was stored at 4 °C for 30 min to form the first dual physically cross-linked network. After that, the glass mold was put under an ultraviolet (UV) lamp (wavelength: 365 nm, intensity: 8 W) for 1 h to obtain the second network of pHEAA. The as-prepared DN gels were named as DN-G_m-H_m-K_c, where G_m, H_m, and K_c represented the mass of κ -CG in mg, the mass of HEAA in g, the concentration of K⁺ in wt % (relative to the κ -CG), respectively. A series of DN-G_m-H_m-K_c gels has been prepared and the preparation conditions were summarized in Table S1. To make comparison, the κ -CG SN gels, κ -CG-K⁺ SN gels, and pure pHEAA SN gels were prepared using a similar approach. The κ -CG SN gels and κ -CG-K⁺ SN gels were prepared via a heating-cooling procedure induced sol-gel process. The pure pHEAA SN gels were directly synthesized by photopolymerization without adding of κ -CG and K⁺. The DN-G₂₀₀-H₅-K₆@NaSCN gels were prepared similar with the DN-G₂₀₀-H₅-K₆ gels, except for using a hydrogen-bonding breaking solvent of 5.0 M NaSCN solution as solvent instead of water.

2.3. Characterizations

Fourier transform infrared (FT-IR) spectrometer (Nicolet Is10, USA) was performed to detect the chemical components of the hydrogels. The microstructure of the DN gels was observed using an emission scanning electron microscope (SEM, JSM-6380LV, Tokyo, Japan). Before the observation, the DN gels samples were frozen by liquid nitrogen, then lyophilized in a vacuum freeze dryer. The surface morphologies of the DN gels were investigated after gold sputter coating. The transmittance

of the DN gels with thickness of 1 mm was determined by UV adsorption spectrum obtained on a UV-vis spectrophotometer (Shimadzu, UV 1800).

2.4. Mechanical tests

Tensile Tests. For uniaxial tensile measurements, a universal tensile testing machine was used to test the dumbbell shape hydrogels (the length of 25 mm, width of 3.18 mm, and thickness of 1 mm) at a speed of 100 mm/min and a load of 100 N. Tensile strength (σ) was the load force at the break divided by the original cross-sectional area of the dumbbell-shaped hydrogels. Tensile strain (ϵ) was the ratio of the tensile length to the original length of the hydrogel specimen. Elastic modulus was obtained by linear fitting based on the approximate straight line part of the stress-strain curve (strain range of 10–30%).

Hysteresis Tests. The energy dissipation of the hydrogels was evaluated by successive loading-unloading experiments. Dissipated energy was estimated from the area between the loading-unloading curves.

Tearing Tests. The samples which were cut into the shape of trousers (40 mm in length, 25 mm in width, and 1 mm in thickness) with an initial notch of 20 mm were used to perform the tearing test. The two arms were respectively clamped on both ends of the universal tensile machine and stretched at 100 mm/min. The tearing energy (T) was defined as the work required per unit tearing area and estimated by $T = 2F_{\max}/\omega$, where F_{\max} was the maximum force value of the tearing process and ω was the thickness of the hydrogels sample.

Self-Healing Tests. The specimens were completely cut into two parts and then the cut sections were brought together. The contacted hydrogels coated with a thin layer of vacuum-fat were rested at room temperature or 95 °C for 12 h.

Shearing Tests. The sandwich-like of hydrogel samples was used for shear testing, which consists of two microscope slides (75 mm \times 25 mm \times 1 mm) and 1 mm of hydrogels between two slides. Each side of the glass was clamped, with one clamped up at a constant crosshead speed and the other held. The maximum adhesive strength was determined by dividing the maximum force in the shearing process by the contact area between the hydrogels and the glass.

Peeling Tests. The adhesion property of the hydrogels (length of 120 mm, width of 12 mm, and thickness of 3 mm) was studied by the 90° peeling experiment. Before the test, solid substrates of various materials were successively cleaned with acetone, ethanol, and water in ultrasound machines for 30 min and dried in an oven. The samples were then prepared on a clean substrate using a heat-resistant silicone mold and a transparent PET film. Finally, peeling measurements were carried out at the crosshead speed of 50 mm/min. The adhesion strength was defined as the maximum force in the peeling process divided by the width of the hydrogels.

Swelling Tests. The swelling properties of hydrogels were evaluated by the gravimetric method. The hydrogels were completely and separately immersed in water, NaSCN (5.0 M), and urea solution (5.0 M). At intervals, the hydrogels after removing excess water from the surface were weighed. The swelling ratio (SR) was estimated by an equation of $SR_{(g/g)} = (m_t - m_0)/m_0$, where m_0 was the original weight of specimens and m_t was the weight of hydrogels after different swelling times.

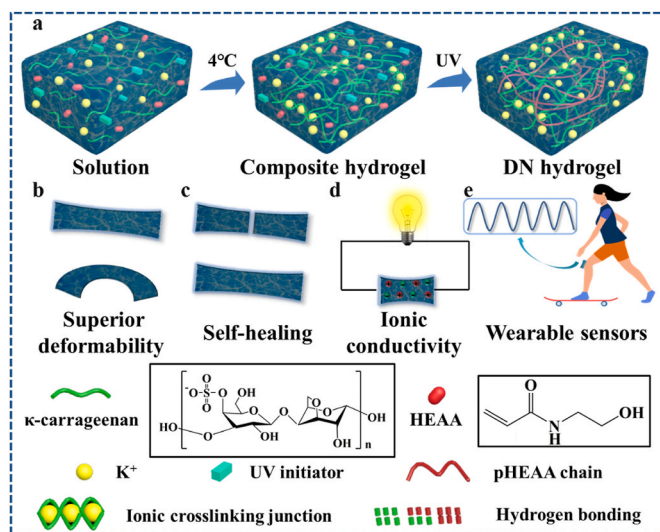
Strain Responsiveness Tests. The strain responsiveness of the hydrogel was tested by the combination of a universal tensile testing machine (E44.104, MTS, China) and a CHI400C type electrochemical workstation at a constant voltage of 1 V. To test the sensitivity of hydrogel sensors to a variety of human activities, hydrogels were attached to human bodies, such as knees and elbows, and then connected to electrochemical workstations. Polarization current-time diagrams were obtained by using chronoamperometry.

3. Results and discussion

3.1. Synthesis and characterization of κ -CG- K^+ /pHEAA DN gels

Briefly, the fully physically crosslinked κ -CG- K^+ /pHEAA DN gels were prepared by a simple heating-cooling-photopolymerization process as shown in Scheme 1a. Upon mixing all reactants of κ -CG, HEAA monomer, KCl, and UV initiator (Irgacure 2959) in water, a homogeneous precursor solution was obtained, then heated up to 95 °C, and gradually cooled down to room temperature. After the heating-cooling process, the first physically crosslinked κ -CG- K^+ network was formed due to the thermo-reversible sol-to-gel of κ -CG and the metal coordination between K^+ and κ -CG [40]. Meanwhile, HEAA monomers and UV initiators were incorporated in the κ -CG- K^+ network. Then, UV light was applied to the solution for initiating the HEAA polymerization to form the second pHEAA network, which was interpenetrated into the κ -CG- K^+ network. Due to the presence of significant hydroxyl groups in both κ -CG and pHEAA chains, hydrogen bonds between pHEAA chains and κ -carrageenan macromolecules serve as additional physical bonds to crosslink pHEAA and κ -carrageenan, thus producing the two physically crosslinked networks in κ -CG- K^+ /pHEAA DN gels. The as-prepared κ -CG- K^+ /pHEAA double-network hydrogels have combined merits of excellent mechanical properties, self-healing properties, ionic conductivity and adhesion properties, which can be fabricated as wearable strain sensors for human motion monitoring (Scheme 1b-e).

To confirm the successful synthesis of κ -CG- K^+ /pHEAA DN gels, comparative FTIR characterizations of κ -CG SN hydrogels, κ -CG- K^+ SN hydrogels, pHEAA SN hydrogels, and κ -CG- K^+ /pHEAA DN gels were performed. Using DN-G₂₀₀-H₅-K₆ gels as a typical example of the κ -CG- K^+ /pHEAA DN gels whose preparation conditions were listed in Table S1. FTIR spectra showed that κ -CG SN hydrogels presented three typical peaks at 1070, 924, and 846 cm^{-1} , assigning to the C–O of dehydrated galactose, C–O–C of 3, 6-dehydrated D-galactose, and C₄–O–S stretch vibrations in κ -CG, respectively [41]. (Fig. 1a). For comparison, κ -CG SN gel also presented a characteristic peak at 1262 cm^{-1} corresponding to the symmetric stretching vibration of O=S=O ($-OSO_3^-$), which was shifted to 1251 cm^{-1} for κ -CG- K^+ SN hydrogels (Fig. 1a). This indicates the metal coordination between the K^+ and κ -CG in κ -CG- K^+ SN hydrogels [42]. Comparison of the FTIR spectrum between DN-G₂₀₀-H₅-K₆ DN gels and pHEAA SN gels showed that the absorption peaks at 1644 cm^{-1} (amide, C=O stretching vibration) and



Scheme 1. (a) Synthesis route of the fully physically crosslinked κ -CG- K^+ /pHEAA DN gels. (b) Mechanical properties, (c) self-healing properties, and (d) ionic conductivity of the κ -CG- K^+ /pHEAA DN gels. (e) Wearable strain sensor for human motion monitoring.

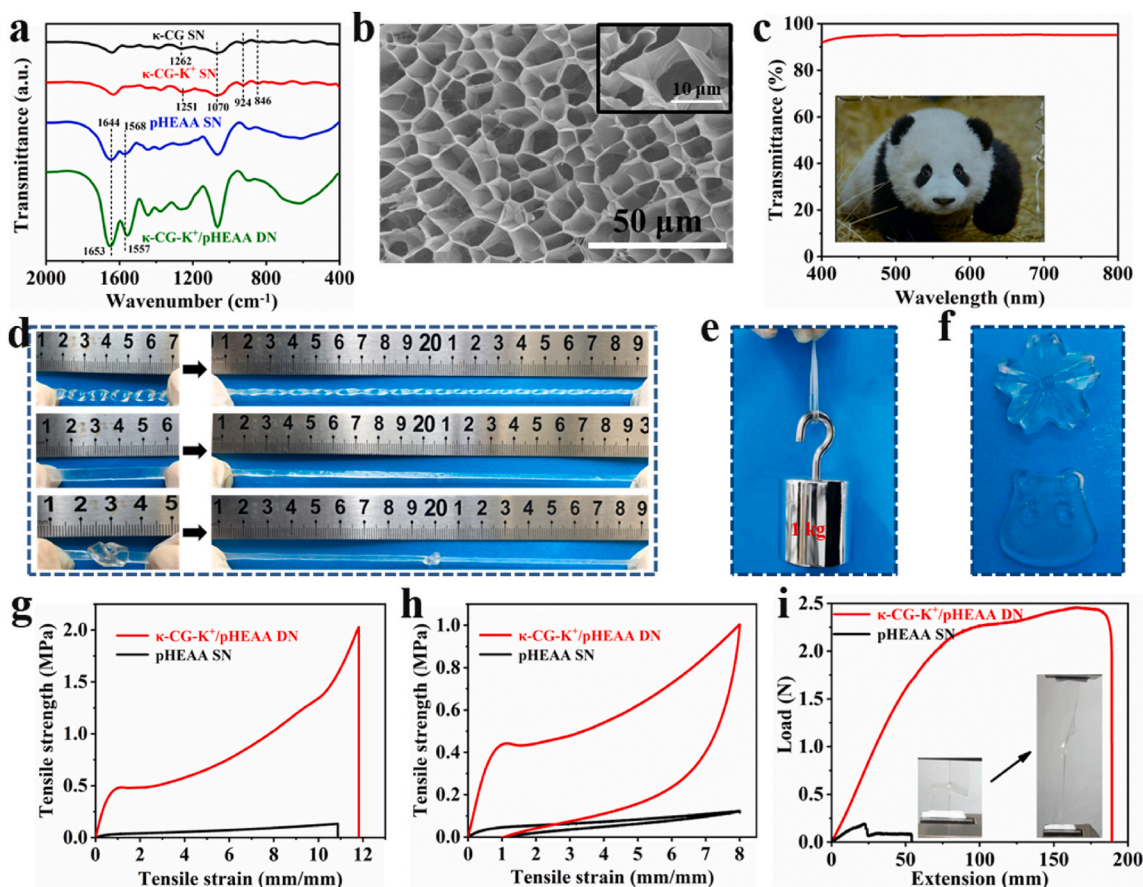


Fig. 1. (a) FTIR spectra of κ -CG SN hydrogels, κ -CG- K^+ SN hydrogels, pHEAA SN hydrogels, and DN- G_{200} - H_5 - K_6 gels. (b) SEM image of DN- G_{200} - H_5 - K_6 gels with high magnification in inset. (c) Optical transmittance of DN- G_{200} - H_5 - K_6 gels and clear visualization of the gels on the top of a panda image. Visual inspection of mechanical properties of DN- G_{200} - H_5 - K_6 gels by (d) twisted stretching, normal stretching, and knotted stretching, (e) holding a weight of 1 kg, (f) forming of different shapes. Side-by-side comparison of (g) tensile property, (h) hysteresis loop, and (i) tearing energy between DN- G_{200} - H_5 - K_6 gels and pHEAA SN hydrogels.

1568 cm^{-1} (amide, N-H bending vibration) in pHEAA SN gels were shifted to 1653 cm^{-1} and 1557 cm^{-1} in DN- G_{200} - H_5 - K_6 DN gels [32], suggesting the formation of hydrogen bonds between κ -CG- K^+ and pHEAA chains. In parallel, SEM images at different magnification showed that the DN- G_{200} - H_5 - K_6 gels appeared a dense and uniform porous structure with pore sizes of 8–11 μm (Fig. 1b). UV spectra demonstrated the high transparency of DN- G_{200} - H_5 - K_6 gels with optical transmittance of 91% in the range of 400–800 nm (Fig. 1c).

The mechanical properties of the DN- G_{200} - H_5 - K_6 gels were qualitative and quantitative researched. At a first glance, the as-prepared DN- G_{200} - H_5 - K_6 gels (size: 5 mm \times 55 mm \times 3 mm) presented excellent mechanical properties, enabling to withstand stretching, twisted stretching, and knotted stretching (Fig. 1d), hold a weight of 1 kg (Fig. 1e), and can form a variety of complex flowers and bear patterns (Fig. 1f). Quantitatively, DN- G_{200} - H_5 - K_6 gels exhibited high tensile strength of 2.02 MPa, elastic modulus of 0.79 MPa, tensile strain of 1181%, dissipated energy of 3259 kJ/m^3 , and the tearing energy of 4917 J/m^2 (Fig. 1g–i and Figs. S1a–b), in sharp contrast to the much weak mechanical properties of pHEAA SN hydrogels (tensile strength of 0.12 MPa, elastic modulus of 0.05 MPa, tensile strain of 1088%, dissipated energy of 199 kJ/m^3 , and tearing energy of 596 J/m^2). The excellent mechanical properties of DN- G_{200} - H_5 - K_6 gels were mainly attributed to the double network structure with contrasting mechanical properties [43]. When subjected to external forces, the first, rigid, and brittle polysaccharide network in the DN gels was fractured and acted as the sacrifice bond to dissipate energy, while the second, soft, and elastic pHEAA still retained intact to maintain high mechanical properties.

3.2. Mechanical properties of κ -CG- K^+ /pHEAA DN gels

Generally, the network compositions are the key determinators for the mechanical properties of κ -CG- K^+ /pHEAA DN gels [36,42,44]. Herein, we examined the effects of network compositions of κ -CG (m_{CG}), K^+ (C_{K^+}), and HEAA (m_{HEAA}) on tensile properties of different κ -CG- K^+ /pHEAA DN gels, whose preparation conditions were summarized in Table S1. Firstly, we studied the effect of m_{CG} on the mechanical properties of κ -CG- K^+ /pHEAA DN gels. As shown in Fig. 2a–b and Table S1, as m_{CG} increased from 75 to 200 mg, κ -CG- K^+ /pHEAA DN gels increased their tensile strength from 1.43 to 2.02 MPa, elastic modulus from 0.15 to 0.79 MPa, but tensile strain decreased from 1550 to 1181%. The higher m_{CG} tended to toughen κ -CG- K^+ /pHEAA DN gels due to the rigid nature of κ -CG. However, the continuous increase of m_{CG} above 200 mg led to an extreme difficulty to form a homogeneous solution for preparing κ -CG- K^+ /pHEAA DN gels. Thus, we determined an optimal m_{CG} of 200 mg to prepare κ -CG- K^+ /pHEAA DN gels with balanced and better mechanical properties for later tests.

Second, in the case of the K^+ concentration (C_{K^+}) effect in Fig. 2c, as the C_{K^+} increased from 0 wt% to 6 wt%, κ -CG- K^+ /pHEAA gels increased tensile strength/tensile strain from 1.20 MPa/1102% to 2.02 MPa/1181%. However, further increase of C_{K^+} to 9 wt% led to the decrease of tensile strength/tensile strain to 1.90 MPa/1038% (Fig. 2d and Table S1), suggesting the over-crosslinking effect of K^+ , which promotes ionic solvation and crosslinking, but competitively reduce the number of hydrogen bonds between κ -CG and pHEAA chains [45]. Differently, since elastic modulus was mainly determined by the first κ -CG- K^+ network, elastic modulus monotonically increased from 0.40 to 0.91

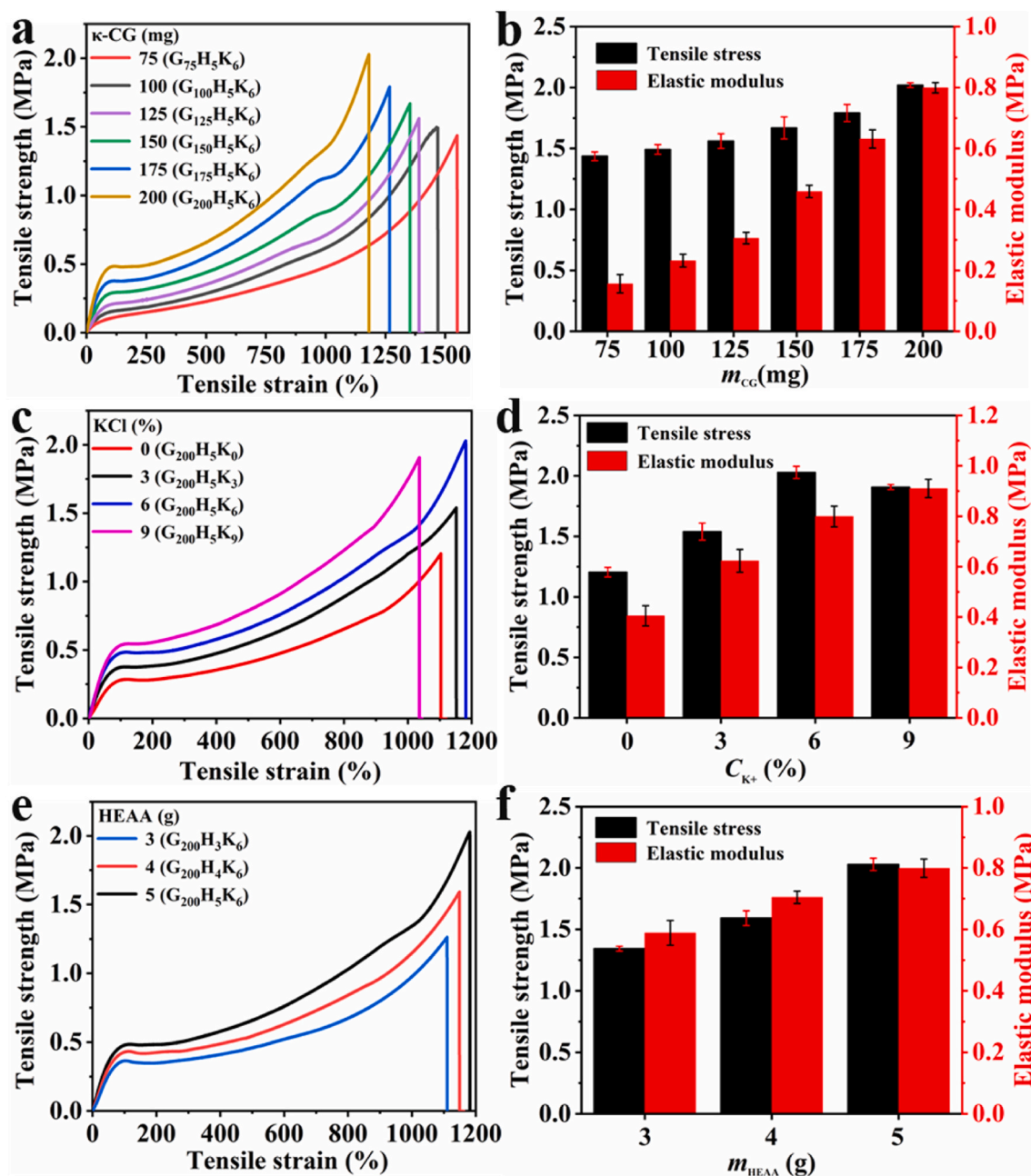


Fig. 2. Tensile strength-strain curves and the corresponding tensile values of κ -CG- K^+ /pHEAA DN gels prepared at different (a–b) m_{CG} , (c–d), C_{K^+} , and (e–f) m_{HEAA} .

MPa as C_{K^+} , an indicator of C_K -induced high crosslinking density. Thus, C_{K^+} of 6 wt% was used to prepare κ -CG- K^+ /pHEAA gels for the following tests.

Third, regarding the HEAA (m_{HEAA}) effect, Fig. 2e shows the strain-stress curves of the κ -CG- K^+ /pHEAA DN gels prepared at different m_{HEAA} . It can be seen that as m_{HEAA} increased from 3.0 to 5.0 g, κ -CG- K^+ /pHEAA DN gels increased tensile strength from 1.26 to 2.02 MPa, elastic modulus from 0.58 to 0.79 MPa, and tensile strain from 1111% to 1181% (Fig. 2f and Table S1). Due to the intrinsic soft and elastic nature of pHEAA, the higher m_{HEAA} will generate more pHEAA chains to enhance not only the crosslinking density of the second network but also chain entanglement between and within two networks. Of note, the gels cannot be well prepared as m_{HEAA} of >5.0 g, because the high m_{HEAA} affects solvent polarity and thus reduces the solubility of κ -CG in water. Based on the results above, DN- G_{200} - H_5 - K_6 gels prepared at the optimal conditions ($m_{CG} = 200$ mg, $C_{K^+} = 6$ wt%, $m_{HEAA} = 5.0$ g) enabled to

achieve tensile strength of 2.02 MPa, tensile strain of 1180%, and elastic modulus of 0.79 MPa and will be used for subsequent studies.

3.3. Energy dissipation and self-healing properties of κ -CG- K^+ /pHEAA DN gels

Energy dissipation of DN- G_{200} - H_5 - K_6 gels was evaluated by continuous loading-unloading cycles, during which no resting time between any two-consecutive loading cycles [46]. As shown in Fig. 3a–b, DN- G_{200} - H_5 - K_6 gels presented the increased hysteresis loops as the tensile strain increased from 50% to 900%, and accordingly dissipated energy increased from 0.10 MJ/m³ to 1.56 MJ/m³. It can be also observed that small fracture energy was dissipated through the first κ -CG- K^+ network at small tensile strains of <250% [36], which is likely to break ionically crosslinkers of κ -CG into small clusters as evidenced by the onset of necking. Meanwhile, high tensile strains of >250% led to

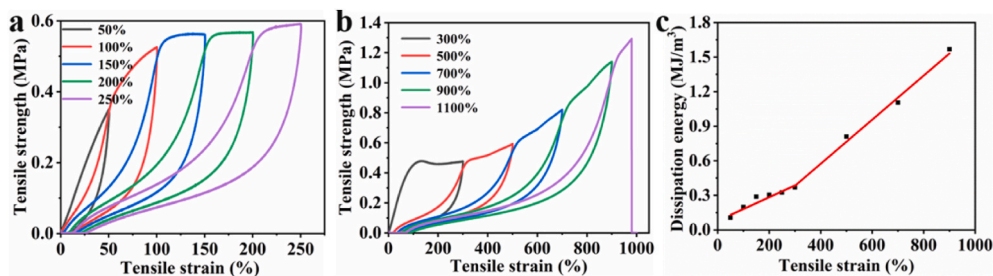


Fig. 3. Hysteresis loops of DN-G₂₀₀-H₅-K₆ gels at (a) small strains of 50–250% and (b) large strains of 300–1100% using cyclic loading-unloading tests. (c) The corresponding dissipated energy of DN-G₂₀₀-H₅-K₆ gels at different strains, as calculated from hysteresis loops from (a) and (b).

large dissipated energy as required to break additional hydrogen bonds between κ -CG-K⁺ and pHEAA chains, as well as the strong associations between small κ -CG clusters and flexible pHEAA chains. The swelling experiments performed in water, urea solution (5.0 M), and NaSCN solution (5.0 M) demonstrated that hydrogen bonding was considered as the major noncovalent interaction in κ -CG-K⁺/pHEAA DN gels by comparing the swelling degree and the mechanical strength of the swelling equilibrated hydrogels, as discussed in Fig. S2.

Due to the reversible nature of network interactions in κ -CG-K⁺/pHEAA hydrogels, we challenged DN-G₂₀₀-H₅-K₆ gels for their self-healing property. A single gel was cut into two parts, with one cut piece being dyed by crystal violet for eye guidance. Then, the two cut parts were put together without any external force. After resting the cut gels at 95 °C for 12 h, the cut gel pieces were well adhered to each other and become a single gel again. More importantly, the self-healed gel can still withstand a certain degree of stretching, as shown in Fig. 4a, indicating the good self-healing property of κ -CG-K⁺/pHEAA DN gels. Quantitatively, Fig. 4b shows the tensile property of the self-healed gels. It can be seen that the self-healed DN gels still achieved the high tensile strength of 0.75 MPa at tensile strain of 90%. Comparatively, we also

test the tensile strength of the self-healed DN-G₂₀₀-H₅-K₆@NaSCN gels (note : DN-G₂₀₀-H₅-K₆@NaSCN gels means DN-G₂₀₀-H₅-K₆ gels prepared in a hydrogen-bonding breaking solvent of 5.0 M NaSCN solution as depicted in ESI), which was only 88 kPa at tensile strain of 22% after resting at 95 °C for 12 h (Fig. S3). The results suggested that the self-healing property of the DN-G₂₀₀-H₅-K₆ gels was mainly driven by the thermo-reversible gelation behavior of κ -CG and the hydrogen bonding between the κ -CG and pHEAA polymer chains. In addition, the conductivity of the self-healed DN gels was tested in this electrical circuit. As shown in Fig. 4c, when the gel was cut in half, the light was off, but when the two cut gels were put together and self-healed, the light was turned on again, indicating that ionic transformation pathways are completely restored. This cutting-and-self-healing process for the light on/off can be repeated multiple times without any failure (Fig. 4d).

3.4. Surface adhesive of κ -CG-K⁺/pHEAA DN gels

As a flexible strain sensor, it is a mandatory condition to empower the gels with good surface adhesion properties for practical uses. Generally speaking, the interfacial toughness of hydrogels (namely surface

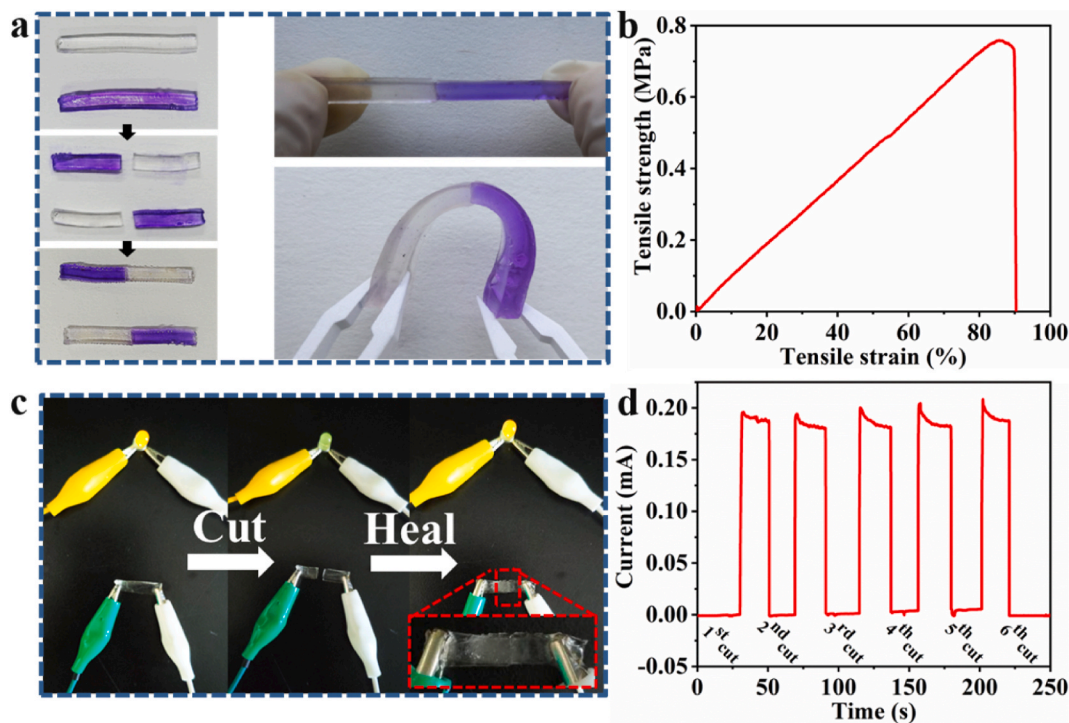


Fig. 4. (a) Visualization of the self-healing of DN-G₂₀₀-H₅-K₆ gels experienced 12 h of resting at 95 °C. (b) The strength-strain curves of the self-healed DN-G₂₀₀-H₅-K₆ gels. (c) Illuminance variation of an LED light during hydrogel cutting/healing. The red rectangle represents the healing region of the DN-G₂₀₀-H₅-K₆ gels. (d) The real-time current change with the cutting and healing of the DN-G₂₀₀-H₅-K₆ Gels for five cycles. (For interpretation of the references to colour in this figure legend, the reader is referred to the Web version of this article.)

adhesion strength) depends mainly on two aspects: the mechanical strength of hydrogels themselves and interfacial interactions between surface and hydrogels [29,34,47]. Upon demonstration of high bulk toughness of κ -CG- K^+ /pHEAA gels, here we aim to test the surface adhesive capacity of the gels. Obviously, the DN-G₂₀₀-H₅-K₆ gels can easily adhere to different untreated surfaces and hold their weights including wood, ceramics, paper, plastic, glass, and steel (Fig. 5a). Additionally, DN-G₂₀₀-H₅-K₆ gels can not only firmly adhere to the human skin of the authors (Fig. 5b), but also easily peel off from the skins without causing pains. Such outstanding surface adhesive property was mainly due to a combination of noncovalent interfacial interactions including hydrogen bonding, van der Waals interactions, and metal complexation between the hydrogels and different surfaces, as stemmed from the rich-functional groups of hydroxyl group (–OH), O–glycosidic bonds, sulfate ester in κ -CG, and plenty of hydroxyl group (–OH), amide group (–CONH–) in pHEAA polymer chains.

Quantitatively, we used a lap shearing test to measure the interfacial

toughness of DN-G₂₀₀-H₅-K₆ gels on nonporous glass. Before the shearing test, the gels were sandwiched in two pieces of glass slide as shown in Fig. 5c. By pulling up the upper glass slide at a constant crosshead speed of 50 mm/min, a typical shear stress extension curve in Fig. S4 showed that DN-G₂₀₀-H₅-K₆ gels exhibited shearing strength of 222 kPa, which was approximately 5-time higher than that of pHEAA SN gels (47 kPa). The poor adhesive property of pHEAA SN gels is mainly attributed to their low mechanical strength of 0.12 MPa [29]. Furthermore, we examined the effect of shearing rates on the shearing strength of DN-G₂₀₀-H₅-K₆ gels on glass. In Fig. 5d-e, the increase of shearing rate from 5 to 100 mm/min led to the shearing strength of DN-G₂₀₀-H₅-K₆ gels from 222 to 505 kPa. This phenomenon indicates that the low shearing rates allow the gels to have sufficient time for relaxing the glass-gel interface and thus for maximizing the energy dissipation as induced by mechanical hysteresis. To confirm interfacial toughness results, we used the 90° peeling test to assess the adhesion strength of DN-G₂₀₀-H₅-K₆ gels on the different surfaces (titanium, aluminum,

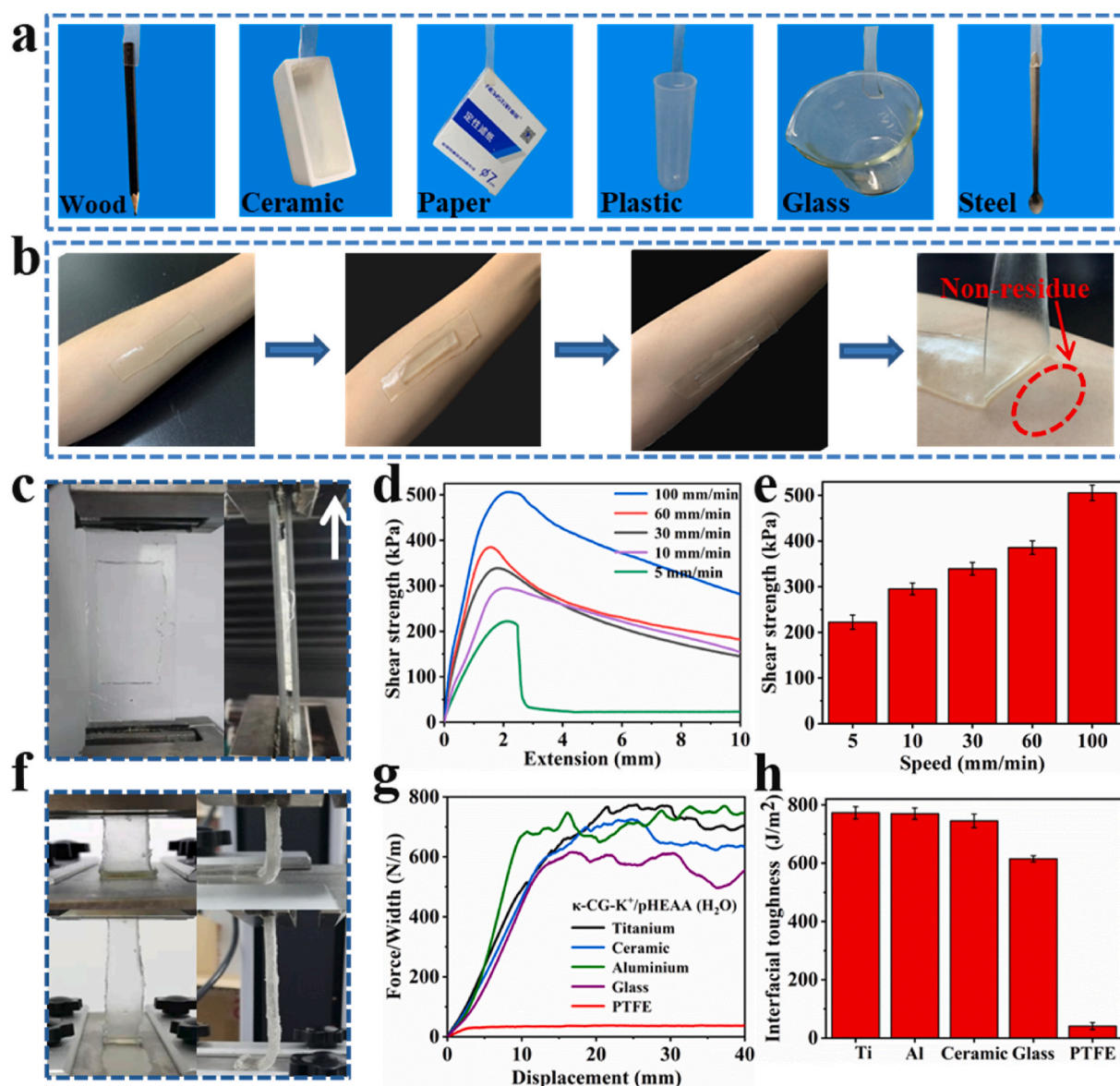


Fig. 5. (a) Typical photographs to show a general surface adhesion of DN-G₂₀₀-H₅-K₆ gels on different solid surfaces of wood, ceramic, paper, glass, and steel. (b) Typical photographs to show the adhesion and peeling off of DN-G₂₀₀-H₅-K₆ gels on human skin. (c) Experimental apparatus for shearing tests of hydrogels adhered between two glass slides, with the adhesion results of (d) shear strength-extension curves and (e) the corresponding shear strength at the different shearing rates. (f) Visual inspection of the 90° peeling-off process. (g) The peeling curves of DN-G₂₀₀-H₅-K₆ gels on different nonporous solid substrates at a speed of 50 mm/min, and (h) the corresponding interfacial toughness.

ceramic, glass, and Teflon). Fig. 5f shows a typical peeling process of DN-G₂₀₀-H₅-K₆ gels from the titanium, while Fig. 5g shows the force-displacement curves of DN-G₂₀₀-H₅-K₆ gels on various substrates at a peeling rate of 50 mm/min. DN-G₂₀₀-H₅-K₆ gels exhibited high adhesion on hydrophilic surfaces of titanium, aluminum, ceramic, and glass with interfacial toughness of 773, 770, 745, and 615 J/m², respectively. In contrast, the interfacial toughness of DN-G₂₀₀-H₅-K₆ gels on hydrophobic Teflon (PTFE) surface was only 41 J/m² (Fig. 5h), simply because hydrogen bonds cannot be formed between hydrogels and hydrophobic PTFE surface.

To test the hypothesis of the important role of hydrogen bonds in surface adhesion, we also measured the interfacial toughness of DN-G₂₀₀-H₅-K₆@NaSCN gels upon peeling them off from the surfaces. The peeling-off curves in Figs. S5a–5b showed that the interfacial toughness of DN-G₂₀₀-H₅-K₆@NaSCN gels on titanium, aluminum, ceramic, and glass was significantly reduced to 118, 110, 104, and 96 J/m², respectively, demonstrating the importance of hydrogen bonds between the κ-CG-K⁺/pHEAA DN gels and surfaces in surface adhesion [30]. In addition, we also test the adhesive properties of the κ-CG-K⁺/pHEAA DN hydrogel on Ti substrate after soaked in water for 6 h and the result is shown in Fig. S6. Due to the swelling of the DN gels in water and the destruction of hydrogen bond, the adhesion ability of the DN gels has been reduced to 361 J/m². Moreover, we compared the tensile and adhesion properties of our κ-CG-K⁺/pHEAA DN gels with those of other hydrogels in the literature. As summarized in Fig. 6, our κ-CG-K⁺/pHEAA DN gels achieved the tensile strength of ~2.02 MPa and interfacial toughness of ~773 J/m² on titanium, in which both properties are superior to those of most hydrogels as reported in the literature, including agar/pHEAA hydrogel [30], gelatin/pHEAA hydrogel [32], agar/pAAEE hydrogel [34], P(AA-co-UCAT)-CS hydrogel [48], PEG nanocomposite hydrogel [49], P(AAm/AMPS)-AFPS hydrogel [50], casein/PAM hydrogel [51], PAA-PDA/CNT hydrogel [52], adenine/PAM hydrogel [53], PAA/HACC hydrogel [54], and CS/PAA hydrogel [55].

3.5. Wearable strain sensors based on κ-CG-K⁺/pHEAA DN gels

Considering the presence of K⁺ ions in the interconnected porous structure of DN gels, it is expected that free migration of K⁺ ions in the network structures empowers the gels to possess strain-induced conductivity [55]. To test this hypothesis, we fixed the DN-G₂₀₀-H₅-K₆ gels with both electronic nodes connected to the LED lamp and the battery. It can be seen in Fig. 7a that the gel can readily light up a LED lamp in a closed-loop circuit, more importantly, when gradually stretching of the gels enabled to decrease the brightness of the LED lamp, reflecting the

strain-induced charge transfer resistance in this electrode system. The decrease of LED brightness is likely attributed to the fact that the stretching-induced decrease of cross-section area in the gel leads to the reduction of ions flux across the cross-section, thus lowering electronic conductivity and LED brightness (Fig. 7b). The conductivity of the DN gels was measured to be 0.29 S/m.

Quantitatively, we measured the strain-induced electromechanical sensitivity of DN-G₂₀₀-H₅-K₆ gel using the relative resistance change as a function of strains: gauge factor ($GF = (\Delta R/R_0)/(\Delta L/L_0)$), where R_0 and L_0 represent the resistance and length of the original hydrogels [56,57]. Fig. 7c shows the real-time GF changes when stretching the gel, in which relative resistance monotonically from 0 to 592% as strains increased from 0 to 300%. Accordingly, the estimated GF was 0.96 at small strains of 0–100% and 2.48 at large strains of 100–300%, respectively. Further, the sensing stability of DN-G₂₀₀-H₅-K₆ gel was assessed by five consecutive stretching-releasing cycles at different strains of 5%, 10%, 20%, 40%, 60%, 80%, 120%, 200%, and 300%. As shown in Fig. 7d–f, the relative resistance variations as induced by both small and large strains were almost unchanged without any signal decay at different-scale stretching and releasing, indicating a robust sensing reproducibility as strain sensors [58].

Due to high strain-induced sensitivity and excellent surface adhesiveness of κ-CG-K⁺/pHEAA hydrogels, we further examined the strain-induced sensitivity at the hydrogel-surface interface to monitor different human motions (i.e. this paper author's finger, wrist, elbow, and knee). Firstly, DN-G₂₀₀-H₅-K₆ gels were self-adhered on the index finger of the authors of this paper. The two ends of DN-G₂₀₀-H₅-K₆ gels were fixed by copper sheets being connected to an electrochemical workstation. Fig. 8a recorded the resistance changes of strain sensors upon the bending of the finger. It can be seen that the resistance changes increased in a stepwise way from 0 to 10.93% as the finger was bent from 0 to 90°. Remaining the bending status did not induce any change in relative resistances, indicating good electrical signal stability. After straightening the finger back to the original status, both relative resistances rapidly returned to their baseline. Consistently, the adhesion of DN-G₂₀₀-H₅-K₆ gels on the wrist, elbow, and knee allows us to sense the large-scale human motions of these human joints. Fig. 8b–d showed that the gel-based strain sensors can detect reversible and repeatable motions with similar resistance changes without any signal loss. On the other hand, different joint motions resulted in different resistance variations, showing an increased order of wrist < elbow < knee, i.e., the larger joint motions led to the higher resistance changes. Collective results demonstrated that κ-CG-K⁺/pHEAA hydrogels can be used as strain sensors with high sensitivity, stability, and repeatability to monitor and distinguish the human joint motions at different scales.

4. Conclusions

In this work, we designed and fabricated a fully physically cross-linked κ-CG-K⁺/pHEAA DN hydrogels consisting of K⁺ crosslinked κ-carrageenan as the first network and hydrogen bonding crosslinked pHEAA as the second network. Both networks were associated with ionic coordination and hydrogen bonds. Under optimal preparation conditions, the resultant κ-CG-K⁺/pHEAA DN hydrogels achieved a combination of superior mechanical, self-healing, conductive, and adhesive properties, all of which enabled the hydrogels to be served as self-adhesive, stretching-sensitive strain sensors for detecting different human motions. Specifically, the bulk gels can not only achieve maximal tensile strength of 2.02 MPa, tensile strain of 1180%, elastic modulus of 0.79 MPa, but also self-heal to retain the toughness/strain of 0.75 MPa/90% after 12 h resting at 95 °C. Apart from strong bulk toughness, κ-CG-K⁺/pHEAA hydrogels exhibited a general and strong surface adhesion of ~773 J/m² on different solid and soft surfaces (e.g., glass, titanium, ceramic, aluminum, human skin). Finally, thank to its unique combination of superior mechanical, self-adhesive, and conductive properties, the hydrogels were further designed into strain sensors with high

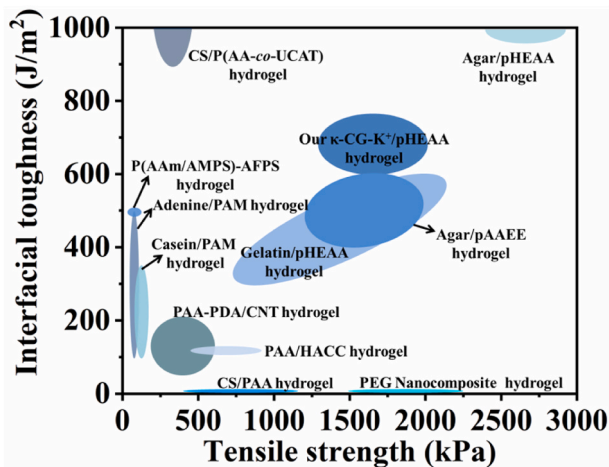


Fig. 6. A summary and comparison of tensile strength and interfacial toughness of our κ-CG-K⁺/pHEAA and other hydrogels as reported in the literature.

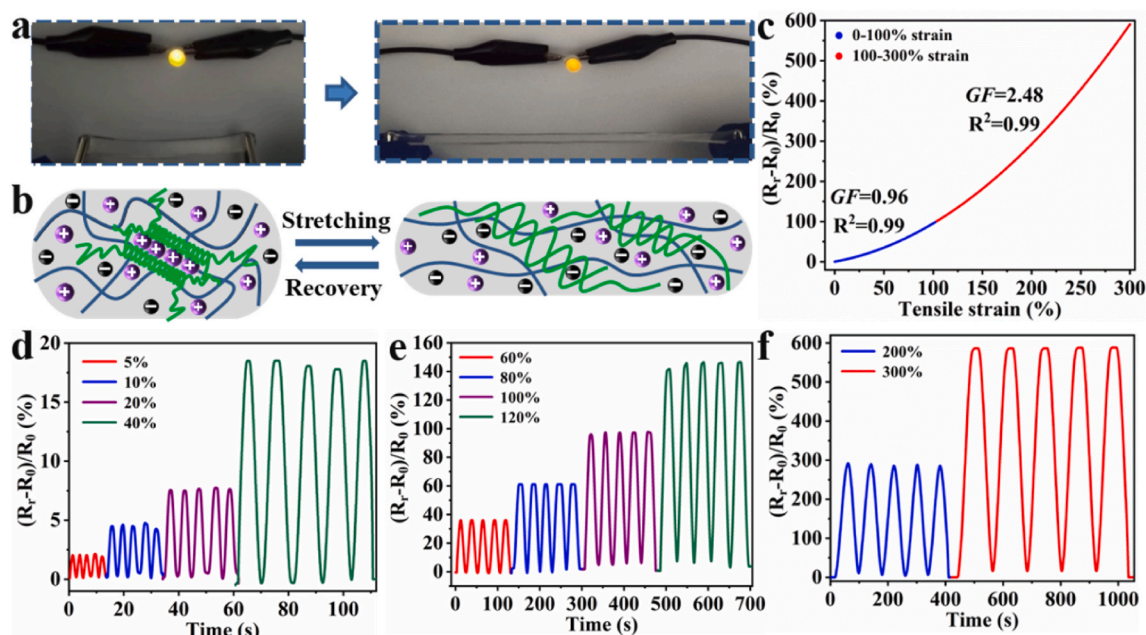


Fig. 7. Strain-induced conductivity and sensitivity of on κ -CG- K^+ /pHEAA DN hydrogels. (a) DN- G_{200} - H_5 - K_6 intact and self-healed gels act as an electric conductor in a closed-loop circuit to light up a LED lamp. (b) Schematic of strain-induced ion flux across the cross-section of the gels during the stretching and releasing processes. (c) Relative resistance changes and gauge factors as a function of applied strains. Relative resistance changes of κ -CG- K^+ /pHEAA-based strain sensors at different strains of (d) 5–40%, (e) 60–120%, and (f) 200–300% during five consecutive stretching-releasing cycles.

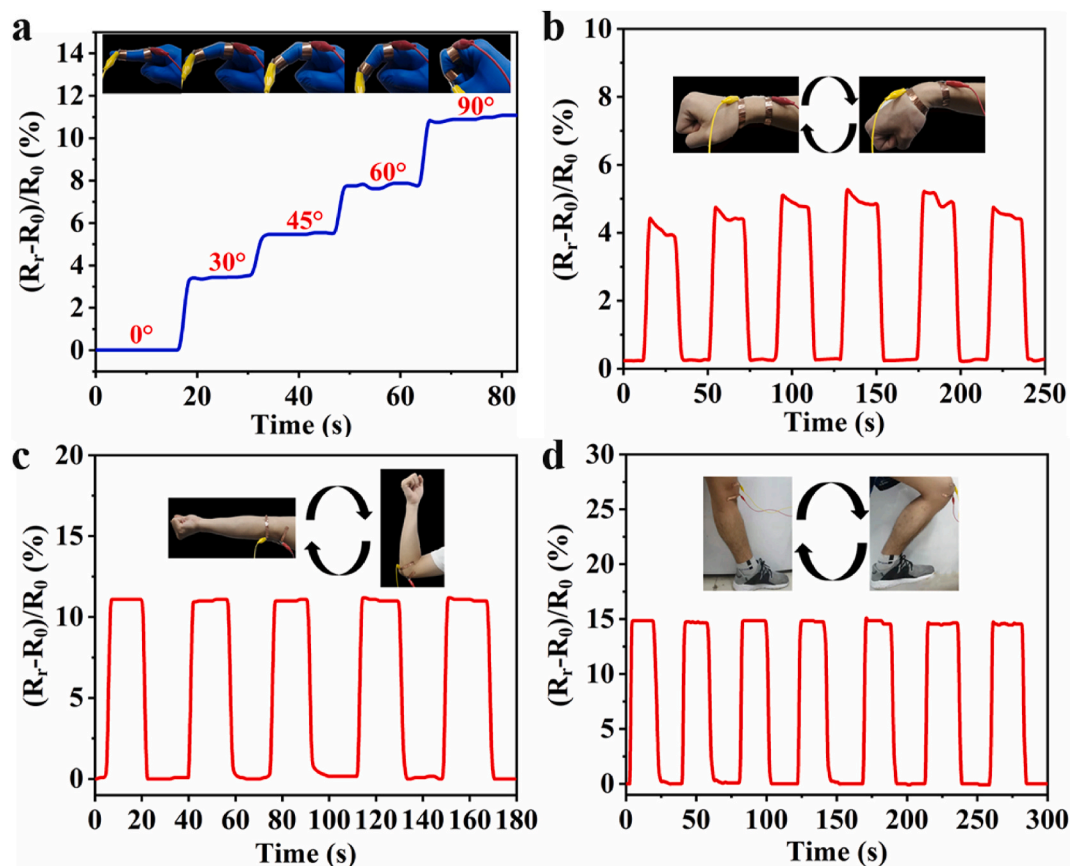


Fig. 8. κ -CG- K^+ /pHEAA hydrogel-based strain sensors for detecting different human joint motions by (a) finger, (b) wrist, (c) elbow, and (d) knee.

sensing stability and robustness for detecting strain-induced human motions by finger, wrist, elbow, and knee. This work provides a new hydrogel system and hydrogel-based strain sensors for broad human-machine interface applications of wearable devices, E-skins, and soft robotics.

CRedit authorship contribution statement

Jianxiong Xu: Project administration, Conceptualization, Writing – original draft, Supervision, Funding acquisition. **Ziyu Guo:** Methodology, Investigation, Data curation. **Yin Chen:** Visualization. **Yuecong Luo:** Formal analysis. **Shaowen Xie:** Software, Validation. **Yutong Zhang:** Data curation. **Haihu Tan:** Resources. **Lijian Xu:** Supervision, Funding acquisition. **Jie Zheng:** Writing – review & editing.

Declaration of competing interest

The authors declare that they have no known competing financial interests or personal relationships that could have appeared to influence the work reported in this paper.

Acknowledgments

The financial support by the National Natural Science Foundation of China (51874129 and 51874128), the Natural Science Foundation of Hunan Province (2020JJ4273), the Scientific Research Fund of Hunan Provincial Education Department (19B153) is gratefully acknowledged. J. Z. thanks financial supports from NSF (CMMI-1825122) and Faculty Summer Fellowship from The University of Akron.

Appendix A. Supplementary data

Supplementary data to this article can be found online at <https://doi.org/10.1016/j.polymer.2021.124321>.

References

- M.H. Liao, P.B. Wan, J.R. Wen, M. Gong, X.X. Wu, Y.G. Wang, R. Shi, L.Q. Zhang, Wearable, healable, and adhesive epidermal sensors assembled from mussel-inspired conductive hybrid hydrogel framework, *Adv. Funct. Mater.* 27 (2017), 1703852, <https://doi.org/10.1002/adfm.201703852>.
- K. Kim, J. Choi, Y. Jeong, I. Cho, M. Kim, S. Kim, Y. Oh, I. Park, Highly sensitive and wearable liquid metal-based pressure sensor for health monitoring applications: integration of a 3D-printed microbump array with the microchannel, *Adv. Healthc. Mater.* 8 (2019), 1900978, <https://doi.org/10.1002/adhm.201900978>.
- W. Chen, Y.H. Bu, D.L. Li, Y. Liu, G.X. Chen, X.F. Wan, N. Li, Development of high-strength, tough, and self-healing carboxymethyl guar gum-based hydrogels for human motion detection, *J. Mater. Chem. C* 8 (2020) 900–908, <https://doi.org/10.1039/C9TC05797H>.
- S. Vanaei, M.S. Parizi, S. Vanaei, F. Saleemizadehparizi, H.R. Vanaei, An overview on materials and techniques in 3D bioprinting toward biomedical application, *Engineered Regeneration* 2 (2021) 1–18, <https://doi.org/10.1016/j.engreg.2020.12.001>.
- M.O. Mansilla, C. Salazar-Hernandez, S.L. Perrin, K.G. Scheer, G. Cildir, J. Toubia, et al., 3D-printed microplate inserts for long term high-resolution imaging of live brain organoids, *BMC Biomedical Engineering* 3 (2021) 3–6, <https://doi.org/10.1186/s42490-021-00049-5>.
- Y.L. Wang, H.L. Huang, J.L. Wu, L. Han, Z.L. Yang, Z.C. Jiang, R. Wang, Z.J. Huang, M. Xu, Ultrafast self-healing, reusable, and conductive polysaccharide-based hydrogels for sensitive ionic sensors, *ACS Sustain. Chem. Eng.* 8 (2020) 18506–18518, <https://doi.org/10.1021/acssuschemeng.0c06258>.
- J. Wang, F. Tang, Y. Wang, Q.P. Lu, S.Q. Liu, L.D. Li, Self-healing and highly stretchable gelatin hydrogel for self-powered strain sensor, *ACS Appl. Mater. Interfaces* 12 (2020) 1558–1566, <https://doi.org/10.1021/acsami.9b18646>.
- V.K. Rao, N. Shauloff, X.M. Sui, H.D. Wagner, R. Jelinek, Polydiacetylene hydrogel self-healing capacitive strain sensor, *J. Mater. Chem. C* 8 (2020) 6034–6041, <https://doi.org/10.1039/D0TC00576B>.
- Z.L. Yang, W.W. Wang, L.L. Bi, L.J. Chen, G.X. Wang, G.N. Chen, C. Ye, J. Pan, Wearable electronics for heating and sensing based on a multifunctional PET/Silver nanowire/PDMS yarn, *Nanoscale* 12 (2020) 16562–16569, <https://doi.org/10.1039/D0NR04023A>.
- Z.H. Yang, Z.R. Zhai, Z.M. Song, Y.Z. Wu, J.H. Liang, Y.F. Shan, J.R. Zheng, H. C. Liang, H.Q. Jiang, Conductive and elastic 3D helical fibers for use in washable and wearable electronics, *Adv. Mater.* 32 (2020), 1907495, <https://doi.org/10.1002/adma.201907495>.
- L. Zhang, H.Q. Li, X.J. Lai, T.Y. Gao, X.R. Zeng, Three-dimensional binary-conductive-network silver Nanowires@Thiolated graphene foam-based room-temperature self-healable strain sensor for human motion detection, *ACS Appl. Mater. Interfaces* 12 (2020) 44360–44370, <https://doi.org/10.1021/acsami.0c13442>.
- Z.W. Wang, Y. Cong, J. Fu, Stretchable and tough conductive hydrogels for flexible pressure and strain sensors, *J. Mater. Chem. B* 8 (2020) 3437–3459, <https://doi.org/10.1039/C9TB02570G>.
- J. Zhang, L.D. Zeng, Z.W. Qiao, J. Wang, X.C. Jiang, Y.S. Zhang, H.H. Yang, Functionalizing double-network hydrogels for applications in remote actuation and in low-temperature strain sensing, *ACS Appl. Mater. Interfaces* 12 (2020) 30247–30258, <https://doi.org/10.1021/acsami.0c13442>.
- Q.H. Wang, X.F. Pan, C.M. Lin, H.L. Gao, S.L. Cao, Y.H. Ni, X.J. Ma, Modified Ti₃C₂T_x (MXene) nanosheet-catalyzed self-assembled, anti-aggregated, ultra-stretchable, conductive hydrogels for wearable bioelectronics, *Chem. Eng. J.* 401 (2020), 126129, <https://doi.org/10.1016/j.cej.2020.126129>.
- H.L. Sun, Y. Zhao, C.F. Wang, K.K. Zhou, C. Yan, G.Q. Zheng, J.J. Huang, K. Dai, C. T. Liu, C.Y. Shen, Ultra-stretchable, durable and conductive hydrogel with hybrid double network as high performance strain sensor and stretchable triboelectric nanogenerator, *Nano Energy* 76 (2020), 105035, <https://doi.org/10.1016/j.nanoen.2020.105035>.
- W.W. Hou, N.N. Sheng, X.H. Zhang, Z.H. Luan, P.F. Qi, M. Lin, Y.Q. Tan, Y.Z. Xia, Y.H. Li, K.Y. Sui, Design of injectable agar/NaCl/polyacrylamide ionic hydrogels for high performance strain sensors, *Carbohydr. Polym.* 211 (2019) 322–328, <https://doi.org/10.1016/j.carbpol.2019.01.094>.
- X. Di, Q.Y. Ma, Y. Xu, M.M. Yang, G.L. Wu, P.C. Sun, High performance ionic conductive poly(vinyl alcohol) hydrogel for flexible strain sensor based on a universal soaking strategy, *Mater. Chem. Front.* 5 (2021) 315–323, <https://doi.org/10.1039/D0QM00625D>.
- T.J. Long, Y.X. Li, X. Fang, J.Q. Sun, Salt-Mediated polyampholyte hydrogels with high mechanical strength, excellent self-healing property, and satisfactory electrical conductivity, *Adv. Funct. Mater.* 28 (2018), 1804416, <https://doi.org/10.1002/adfm.201804416>.
- D. Zhang, B.P. Ren, Y.X. Zhang, L.J. Xu, Q.Y. Huang, Y. He, X.F. Li, J. Wu, J. T. Yang, Q. Chen, Y. Chang, J. Zheng, From design to applications of stimuli-responsive hydrogel strain sensors, *J. Mater. Chem. B* 8 (2020) 3171–3191, <https://doi.org/10.1039/C9TB02692D>.
- P. Calvert, Hydrogels for soft machines, *Adv. Mater.* 21 (2009) 743–756, <https://doi.org/10.1002/adma.200800534>.
- Y.J. Wang, C.Y. Li, Z.J. Wang, Y.P. Zhao, L. Chen, Z.L. Wu, Q. Zheng, Hydrogen bond-reinforced double-network hydrogels with ultrahigh elastic modulus and shape memory property, *J. Polym. Sci. Pol. Phys.* 56 (2018) 1281–1286, <https://doi.org/10.1002/polb.24620>.
- H.L. Sun, K.K. Zhou, Y.F. Yu, X.Y. Yue, K. Dai, G.Q. Zheng, C.T. Liu, C.Y. Shen, Highly stretchable, transparent, and bio-friendly strain sensor based on self-recovery ionic-covalent hydrogels for human motion monitoring, *Macromol. Rapid Comm.* 304 (2019), 1900227, <https://doi.org/10.1002/mame.201900227>.
- X.F. Feng, X.L. Hou, C.J. Cui, S.B. Sun, S. Sadiq, S.H. Wu, F. Zhou, Mechanical and antibacterial properties of tannic acid-encapsulated carboxymethyl chitosan/polyvinyl alcohol hydrogels, *Engineered Regeneration* 2 (2021) 57–62, <https://doi.org/10.1016/j.engreg.2021.05.002>.
- H.T. Zhang, X.J. Wu, Z.H. Qin, X. Sun, H. Zhang, Q.Y. Yu, M.M. Yao, S.S. He, X. R. Dong, F.L. Yao, J.J. Li, Dual physically cross-linked carboxymethyl cellulose-based hydrogel with high stretchability and toughness as sensitive strain sensors, *Cellulose* 27 (2019) 9975–9989, <https://doi.org/10.1007/s10570-020-03463-5>.
- Y.Z. Liang, L.N. Ye, X.Y. Sun, Q. Lv, H.Y. Liang, Tough and stretchable dual ionically cross-linked hydrogel with high conductivity and fast recovery property for high-performance flexible sensors, *ACS Appl. Mater. Interfaces* 12 (2019) 1577–1587, <https://doi.org/10.1021/acsami.9b18796>.
- C. Liu, X.Y. Xu, W.G. Cui, H.B. Zhang, Metal-organic framework (MOF)-based biomaterials in bone tissue, *Engineered Regeneration* 2 (2021) 105–108, <https://doi.org/10.1016/j.engreg.2021.09.001>.
- L. Cheng, Y. Wang, G.M. Sun, S.Z. Wen, L.F. Deng, H.Y. Zhang, W.G. Cui, Hydration-Enhanced lubricating electrospun nanofibrous membranes prevent tissue adhesion, *Research* (2020), 4907185, <https://doi.org/10.34133/2020/4907185>.
- S. Xia, S.X. Song, F. Jia, G.H. Gao, A flexible, adhesive and self-healable hydrogel-based wearable strain sensor for human motion and physiological signal monitoring, *J. Mater. Chem. B* 7 (2019) 4638–4648, <https://doi.org/10.1039/c9tb01039d>.
- H. Yuk, T. Zhang, S.T. Lin, G.A. Parada, X.H. Zhao, Tough bonding of hydrogels to diverse non-porous surfaces, *Nat. Mater.* 15 (2016) 190–196, <https://doi.org/10.1038/NMAT4463>.
- H. Chen, Y.L. Liu, B.P. Ren, Y.X. Zhang, J. Ma, L.J. Xu, Q. Chen, J. Zheng, Super bulk and interfacial toughness of physically crosslinked double-network hydrogels, *Adv. Funct. Mater.* 27 (2017), 1703086, <https://doi.org/10.1002/adfm.201703086>.
- Q. Chen, L. Zhu, C. Zhao, Q.M. Wang, J. Zheng, A robust, one-pot synthesis of highly mechanical and recoverable double network hydrogels using thermoreversible sol-gel polysaccharide, *Adv. Mater.* 25 (2013) 4171–4176, <https://doi.org/10.1002/adma.201300817>.
- L. Tang, D. Zhang, L. Gong, Y.X. Zhang, S.W. Xie, B.P. Ren, Y.L. Liu, Y.F. Yang, G. Y. Zhou, Y. Chang, J.X. Tang, J. Zheng, Double-network physical cross-linking strategy to promote bulk mechanical and surface adhesive properties of hydrogels,

- Macromolecules 52 (2019) 9512–9525. <https://pubs.acs.org/doi/10.1021/acs.macromol.9b01686>.
- [33] H.J. Li, H. Zheng, Y.J. Tan, S.B. Tor, K. Zhou, Development of an ultrastretchable double-network hydrogel for flexible strain sensors, *ACS Appl. Mater. Interfaces* 13 (2021) 12814–12823, <https://doi.org/10.1021/acsami.0c19104>.
- [34] Y.X. Zhang, B.P. Ren, S.W. Xie, Y.Q. Cai, T. Wang, Z.Q. Feng, J.X. Tang, Q. Chen, J. X. Xu, L.J. Xu, J. Zheng, Multiple physical cross-linker strategy to achieve mechanically tough and reversible properties of double-network hydrogels in bulk and on surfaces, *ACS Appl. Polym. Mater.* 1 (2019) 701–713, <https://doi.org/10.1021/acsapm.8b0023>.
- [35] C.Z. Xu, X.S. Zhang, S. Liu, X.W. Zhao, C.Z. Geng, L.L. Wang, Y.Z. Xia, Selected phase separation renders high strength and toughness to polyacrylamide/alginate hydrogels with large-scale cross-linking zones, *ACS Appl. Mater. Interfaces* 13 (2021) 25383–25391, <https://doi.org/10.1021/acsami.1c04577>.
- [36] L.Y. Zhao, Q.F. Zheng, Y.X. Liu, S. Wang, J. Wang, X.F. Liu, Enhanced strength and toughness of κ -carrageenan/polyacrylic acid physical double-network hydrogels by dual cross-linking of the first network, *Eur. Polym. J.* 124 (2020), 109474, <https://doi.org/10.1016/j.eurpolymj.2020.109474>.
- [37] Y. Deng, M. Huang, D. Sun, Y. Hou, Y.B. Li, T.S. Dong, X.H. Wang, L. Zhang, W. Z. Yang, Dual physically cross-linked κ -carrageenan-based double network hydrogels with superior self-healing performance for biomedical application, *ACS Appl. Mater. Interfaces* 10 (2018) 37544–37554, <https://doi.org/10.1021/acsami.8b15385>.
- [38] Z.W. Fan, L.J. Duan, G.H. Gao, Self-healing carrageenan-driven polyacrylamide hydrogels for strain sensing, *Sci. China Technol. Sc.* 63 (2020) 2677–2686, <https://doi.org/10.1007/s11431-020-1682-3>.
- [39] L.J. Zhou, Z.W. Wang, C.S. Wu, Y. Cong, R. Zhang, J. Fu, Highly sensitive pressure and strain sensors based on stretchable and recoverable ion-conductive physically cross-linked double-network hydrogels, *ACS Appl. Mater. Interfaces* 12 (2020) 51969–51977, <https://doi.org/10.1021/acsami.0c15108>.
- [40] L.Q. Li, J.H. Zhao, Y.R. Sun, F. Yu, J. Ma, Ionically cross-linked sodium alginate/ κ -carrageenan double-network gel beads with low-swelling, enhanced mechanical properties, and excellent adsorption performance, *Chem. Eng. J.* 372 (2019) 1091–1103, <https://doi.org/10.1016/j.cej.2019.05.007>.
- [41] M.J. Zhu, L.M. Ge, Y.B. Lyu, Y.X. Zi, X.Y. Li, D.F. Li, C.D. Mu, Preparation, characterization and antibacterial activity of oxidized κ -carrageenan, *Carbohydr. Polym.* 174 (2017) 1051–1058, <https://doi.org/10.1016/j.carbpol.2017.07.029>.
- [42] H.C. Yu, C.Y. Li, M. Du, Y.H. Song, Z.L. Wu, Q. Zheng, Improved toughness and stability of κ -carrageenan/polyacrylamide double-network hydrogels by dual cross-linking of the first network, *Macromolecules* 629–638 (2019) 52, <https://doi.org/10.1021/acs.macromol.8b02269>.
- [43] J.P. Gong, Y. Katsuyama, T. Kurokawa, Y. Osada, Double-network hydrogels with extremely high mechanical strength, *Adv. Funct. Mater.* 15 (2003) 1155–1158, <https://doi.org/10.1002/adfm.200304907>.
- [44] H.C. Yu, H. Zhang, K.F. Ren, Z.M. Ying, F.B. Zhu, J. Qian, J. Ji, Z.L. Wu, Q. Zheng, Ultrathin κ -carrageenan/chitosan hydrogel films with high toughness and anti-adhesion property, *ACS Appl. Mater. Interfaces* 10 (2018) 9002–9009, <https://doi.org/10.1021/acsami.7b18343>.
- [45] B.W. Yang, W.Z. Yuan, Highly stretchable and transparent double-network hydrogel ionic conductors as flexible thermal-mechanical dual sensors and electroluminescent devices, *ACS Appl. Mater. Interfaces* 11 (2019) 16765–16775, <https://doi.org/10.1021/acsami.9b01989>.
- [46] J. Zhang, L.D. Chen, B. Shen, L.Q. Chen, J. Feng, Ultra-high strength poly(N-(2-hydroxyethyl)acrylamide)/chitosan hydrogel with “repelling and killing” bacteria property, *Carbohydr. Polym.* 225 (2019), 115160, <https://doi.org/10.1016/j.carbpol.2019.115160>.
- [47] S.W. Xie, B.P. Ren, G. Gong, D. Zhang, Y. Chen, L.J. Xu, C.F. Zhang, J.X. Xu, J. Zheng, Lanthanide-doped upconversion nanoparticle-cross-linked double-network hydrogels with strong bulk/interfacial toughness and tunable full-color fluorescence for bioimaging and biosensing, *ACS Appl. Nano. Mater.* 3 (2020) 2774–2786, <https://doi.org/10.1021/acsanm.0c00105>.
- [48] X.M. Fan, Y. Fang, W.K. Zhou, L.Y. Yan, Y.H. Xu, H. Zhu, H.Q. Liu, Mussel foot protein inspired tough tissue-selective underwater adhesive hydrogel, *Mater. Horiz.* 8 (2021) 997–1007, <https://doi.org/10.1039/D0MH01231A>.
- [49] Y. Liu, H. Meng, S. Konst, R. Sarmiento, R. Rajachar, B.P. Lee, Injectable dopamine-modified poly(ethylene glycol) nanocomposite hydrogel with enhanced adhesive property and bioactivity, *ACS Appl. Mater. Interfaces* 6 (2014) 16982–16992, <https://doi.org/10.1021/am504566v>.
- [50] J.J. Xu, R.N. Jing, X.Y. Ren, G.H. Gao, Fish-inspired anti-icing hydrogel sensors with low temperature adhesion and toughness, *J. Mater. Chem. A* 8 (2020) 9373–9381, <https://doi.org/10.1039/D0TA02370A>.
- [51] L. Guan, S. Yan, X. Liu, X.Y. Li, G.H. Gao, Wearable strain sensors based on casein-driven tough, adhesive and anti-freezing hydrogels for monitoring human-motion, *J. Mater. Chem. B* 7 (2019) 5230–5236, <https://doi.org/10.1039/C9TB01340G>.
- [52] J.J. Wang, Q. Zhang, X.X. Ji, L.B. Liu, Highly stretchable, compressible, adhesive, conductive self-healing composite hydrogels with sensor capacity, *Chinese J. Polym. Sci.* 38 (2020) 1221–1229, <https://doi.org/10.1007/s10118-020-2472-0>.
- [53] Q. Zhang, X. Liu, X.Y. Ren, L.J. Duan, G.H. Gao, Adenine-mediated adhesive and tough hydrogel based on hybrid crosslinking, *Eur. Polym. J.* 106 (2018) 139–147, <https://doi.org/10.1016/j.eurpolymj.2018.07.018>.
- [54] T. Wang, X.Y. Ren, Y. Bai, L. Liu, G.F. Wu, Adhesive and tough hydrogels promoted by quaternary chitosan for strain sensor, *Carbohydr. Polym.* 254 (2021), 117298, <https://doi.org/10.1016/j.carbpol.2020.117298>.
- [55] C. Cui, C.Y. Shao, L. Meng, J. Yang, High-strength, self-adhesive, and strain-sensitive chitosan/poly(acrylic acid) double-network nanocomposite hydrogels fabricated by salt-soaking strategy for flexible sensors, *ACS Appl. Mater. Interfaces* 11 (2019) 39228–39237, <https://doi.org/10.1021/acsami.9b15817>.
- [56] F.L. He, X.Y. You, H. Gong, Y. Yang, T. Bai, W.G. Wang, W.X. Guo, X.Y. Liu, M. D. Ye, Stretchable, biocompatible and multifunctional silk fibroin-based hydrogels towards wearable strain/pressure sensors and triboelectric nanogenerators, *ACS Appl. Mater. Interfaces* 12 (2020) 6442–6450, <https://doi.org/10.1021/acsami.9b19721>.
- [57] Y. Tan, Y.Y. Zhang, Y.J. Zhang, J. Zheng, H.Q. Wu, Y. Chen, S.M. Xu, J.L. Yang, C. T. Liu, Y. Zhang, Dual cross-linked ion-based temperature-responsive conductive hydrogels with multiple sensors and steady electrocardiogram monitoring, *Chem. Mater.* 32 (2020) 7670–7678, <https://doi.org/10.1021/acs.chemmater.0c01589>.
- [58] H.Y. Liu, X. Wang, Y.X. Cao, Y.Y. Yang, Y.T. Yang, Y.F. Gao, Z.H. Ma, J.F. Wang, W. J. Wang, D.C. Wu, Freezing-tolerant, highly sensitive strain and pressure sensors assembled from ionic conductive hydrogels with dynamic cross-links, *ACS Appl. Mater. Interfaces* 12 (2020) 25334–25344, <https://doi.org/10.1021/acsami.0c06067>.